

## **Supplementary Material**

Isidoros Kampolis, Stavros Triantafyllidis, Vasilios Skliros and Evangelos Kamperis, "Quaternary evolutionary stages of Selinitsa Cave (SW Peloponnese, Greece) revealing sea level changes based on 3D scanning, geomorphological, biological and sedimentological indicators"

Corresponding author: striantafyllidis@metal.ntua.gr; Tel.: +302107724468

### **Analytical Techniques, Tables, Figures**

The mineralogy and texture of the fine-grained deposits and the clogging material was determined by combination of transmitted light optical microscopy, X-ray diffraction (XRD), Scanning Electron Microscopy (SEM), and RAMAN spectroscopy. X-ray diffraction and SEM were carried out at the Laboratory of Mineralogy, Petrology and Economic Geology, Section of Geological Sciences, School of Mining and Metallurgical Engineering, National Technical University of Athens, Greece. X-ray diffraction involved the use of a BRUKER D8 FOCUS X-ray diffractometer with Ni-filtered Cu(K $\alpha$ ) radiation at 40 kV/40 mA operating conditions (with a 2 $\theta$  angle of 3° to 70°). SEM was performed using a JEOL JSM 6380LV scanning electron microscope combined with energy dispersive X-ray spectrometry (OXFORD ISIS Link electron microprobe) and equipped with a JEOL analytical back-scattered electron detector. Operating conditions for the SEM were 20 kV accelerating voltage, 20 mm working distance and 1.0 nA beam current. Counting time for each analysis was 50 s, with 15 s dead time, whereas the MAC Ltd GEO MK II Block of standards was used for instrument calibration during analysis. Confocal Raman spectra were obtained with a Renishaw in Via Reflex micro-Raman at the School of Chemical Engineering, National Technical University of Athens, Greece. The 532-nm excitation wavelength of an Ar+ laser was employed to acquire Raman spectra in the spectral range 100–4,000 cm $^{-1}$ . The analysis of the scattered beam was taken by a 250-mm focal length spectrometer along with a 1,800 lines/mm diffraction grating and a high sensitivity charge-coupled device detector. Raman measurements were performed at a room temperature with backscattering configuration on a LEICA microscope using a solid-state laser as excitation source. The laser beam was focused onto the samples by means of a  $\times 50$  short distance magnification lens. The wavenumber shifts were calibrated by internal Silicon reference at 521 cm $^{-1}$ . Exposure time of 10 sec and two accumulations cycles for each spectrum were chosen.

The cave deposits were also commercially analyzed at ALS Laboratories (Ireland) for major and trace elements (Si, Ti, Al, Fe, Mg, Mn, Ca, K, Na, P, Sr, Cr and Ba) and trace elements (Ba, Ce, Cr, Cs, Dy, Er, Eu, Ga, Ge, Ag, Cd, Co, As, Bi, Hg, Gd, Hf, Ho, La, Lu, Nb, Nd, Pr, Rb, Cu, Li, Mo, In, Re, Sb, Sm, Sn, Sr, Ta, Tb, Th, Tm, U, V, Ni, Pb, Sc, Se, Te, Tl, W, y, Yb, Zr and Zn) using the whole-rock characterization package CCP-PKG01 on > 10 g splits, employing ICP-MS and ICP-AES. The "AMIS0304", "SY-4" and "OREAS 102a" standards were employed by ALS for major elements and the "SY-4", "REE-1", "OGGeo08", "MRGeo08", "OREAS-503c" and "OREAS-602" standards for trace elements analyses. The rock samples were heated at 1000°C for the determination of Loss on Ignition (LOI), and the total sulfur and carbon contents were measured by LECO Furnace analyzer (ALS Codes C-IR07 and S-IR08, respectively) using the "GS910-4", "GS313-8", "LR-LOI2" and "LR-LOI4" standards. The geochemical analyses results and Standard Deviation calculations for the whole suite of elements are given in ESM Table 1.

**Table S1.** Representative major (wt. %) and trace (ppm) element analyses of the fine-grained deposits in Selinitsa Cave.

Sample	1	2	3	4	5	6	7	S.D.
Major elements								
SiO <sub>2</sub>	59.9	57.4	59.5	59.2	59.0	62.2	59.0	1.33
TiO <sub>2</sub>	0.38	0.32	0.37	0.37	0.35	0.41	0.34	0.03
Al <sub>2</sub> O <sub>3</sub>	7.14	6.03	6.84	6.86	6.58	7.69	6.3	0.51
Fe <sub>2</sub> O <sub>3</sub>	2.51	2.25	2.52	2.55	2.36	2.71	2.33	0.15
MgO	5.28	6.17	5.6	5.72	5.75	4.93	5.83	0.37
CaO	7.71	9.61	8.22	8.48	8.67	7.02	8.98	0.78
Na <sub>2</sub> O	0.64	0.53	0.53	0.52	0.52	0.65	0.54	0.05
K <sub>2</sub> O	0.88	0.74	0.88	0.89	0.84	0.97	0.81	0.07
Cr <sub>2</sub> O <sub>3</sub>	0.015	0.011	0.013	0.012	0.012	0.016	0.012	-
MnO	0.02	0.05	0.1	0.13	0.09	0.02	0.05	0.04
P <sub>2</sub> O <sub>5</sub>	0.33	0.17	0.19	0.2	0.18	0.34	0.17	0.07
BaO	0.02	0.02	0.02	0.02	0.02	0.02	0.02	-
LOI	14.1	16	15.45	15.75	15.95	13.6	15.75	0.90
Total	98.93	99.3	100.23	100.7	100.32	100.58	100.13	
C	3.03	3.71	3.1	3.1	3.12	2.57	3.23	0.31
S	0.01	b.d.l.	0.01	0.01	0.01	0.01	0.01	-
Trace elements								
Y	24.4	24.7	27.2	29.8	26.4	26.7	25.1	1.73
Zr	120	112	152	142	109	144	138	15.79
Th	5.47	4.58	5.29	5.23	4.93	5.63	4.64	0.37
Rb	45.8	39	46.6	48.7	44.5	51.9	42.8	3.83
Sr	55.9	58.9	64	67.3	61.3	61.6	61.1	3.34
Nb	8.7	7.7	8.3	8.6	8	9.5	7.8	0.58
Hf	3.3	3.1	3.2	3.2	2.7	3.6	3.2	0.25
Ta	0.6	0.4	0.5	0.8	0.5	0.5	0.4	0.13
Sc	7	6	8	8	7	8	7	0.70
Cr	100	80	90	80	80	110	80	11.25
La	26.2	24.5	28	28.3	26.7	29	24.4	1.69
Ce	40.8	36.9	40.9	41.6	37.8	44.4	36.9	2.60
Pr	5.83	5.48	5.96	6.31	5.52	6.19	5.23	0.37
Nd	22.5	20.4	23.2	24.7	22.6	23.9	21.4	1.35
Sm	4.24	3.78	4.29	4.81	4.51	4.93	4.12	0.37
Eu	0.94	0.93	0.97	1.15	1.06	1.11	1	0.08
Gd	4.1	4.1	4.46	4.66	4.36	4.74	3.99	0.27
Tb	0.6	0.57	0.65	0.64	0.65	0.68	0.57	0.04
Dy	3.67	3.57	4	4.23	3.87	4.04	3.65	0.22
Ho	0.76	0.74	0.78	0.87	0.83	0.83	0.72	0.05
Er	2.29	2.21	2.45	2.46	2.17	2.4	2.18	0.12
Yb	2.18	2.06	2.14	2.36	1.87	2.22	1.82	0.18
Tm	0.3	0.27	0.3	0.38	0.33	0.34	0.29	0.03
Lu	0.31	0.28	0.31	0.38	0.31	0.38	0.28	0.04
ΣREE	114.72	105.79	118.41	122.85	112.58	125.16	106.55	
ΣLREE	100.51	91.99	103.32	106.87	98.19	109.53	93.05	
ΣHREE	14.21	13.8	15.09	15.98	14.39	15.63	13.5	
ΣLREE/ ΣHREE	0.14	0.15	0.15	0.15	0.15	0.14	0.15	
Y/Ho	32.11	33.38	34.87	34.25	31.81	32.17	34.86	
La/Sc	3.74	4.08	3.50	3.54	3.81	3.63	3.49	

b.d.l.: below detection limit

S.D.: Standard Deviation

ΣREE = Σ(La to Lu), ΣLREE = Σ(La to Eu), ΣHREE = Σ(Gd to Lu)

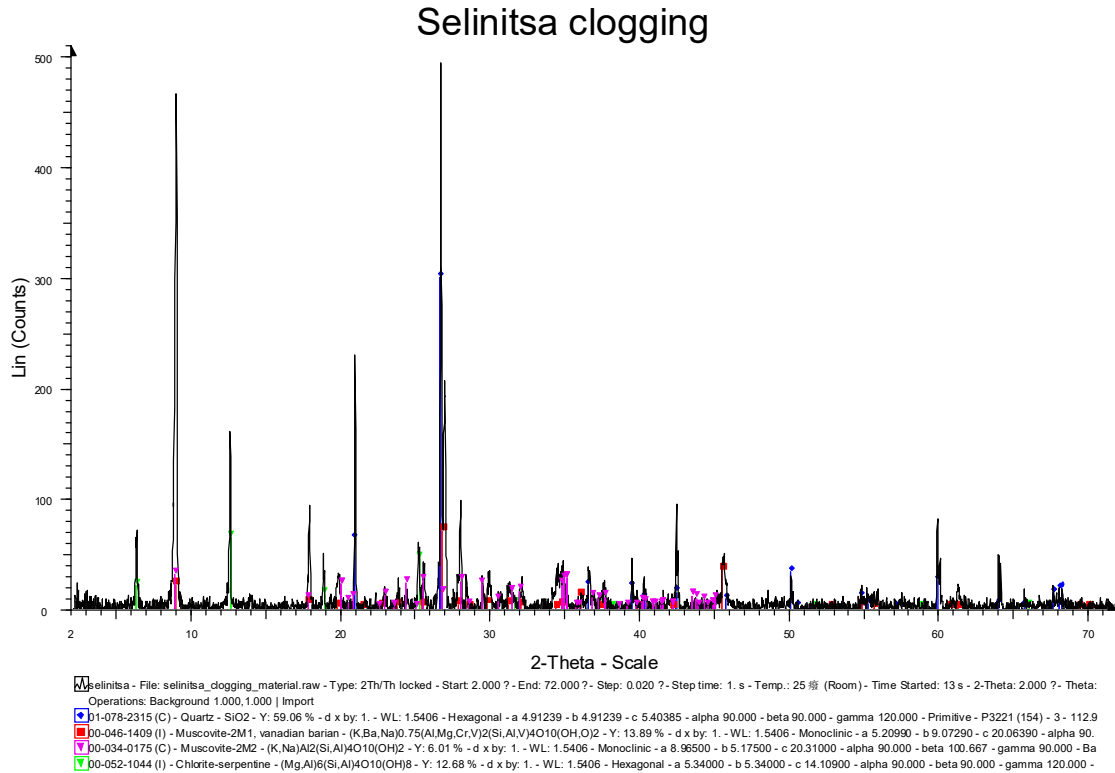


Figure S1: Representative XRD pattern of the clogging material filling cracks, joints, voids and faults in Selinitsa cave.

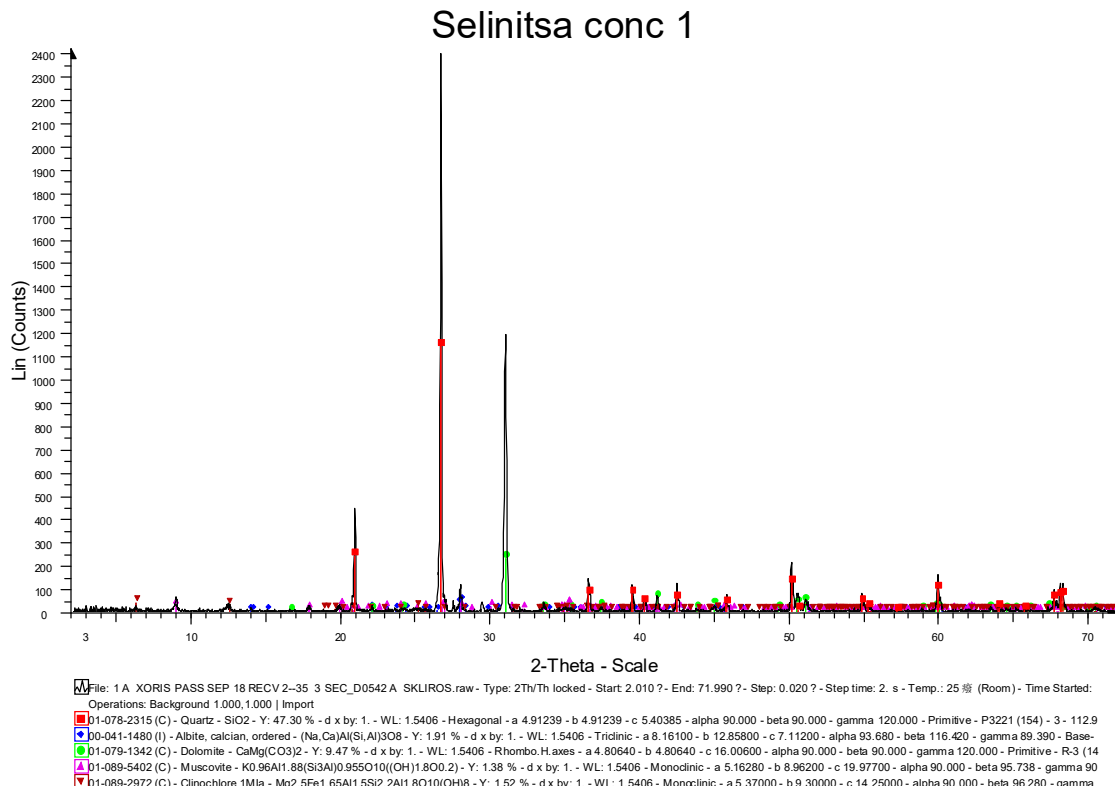


Figure S2: Representative XRD pattern of the fine-grained deposits found in Selinitsa cave.

## Selinitsa concentrate 2

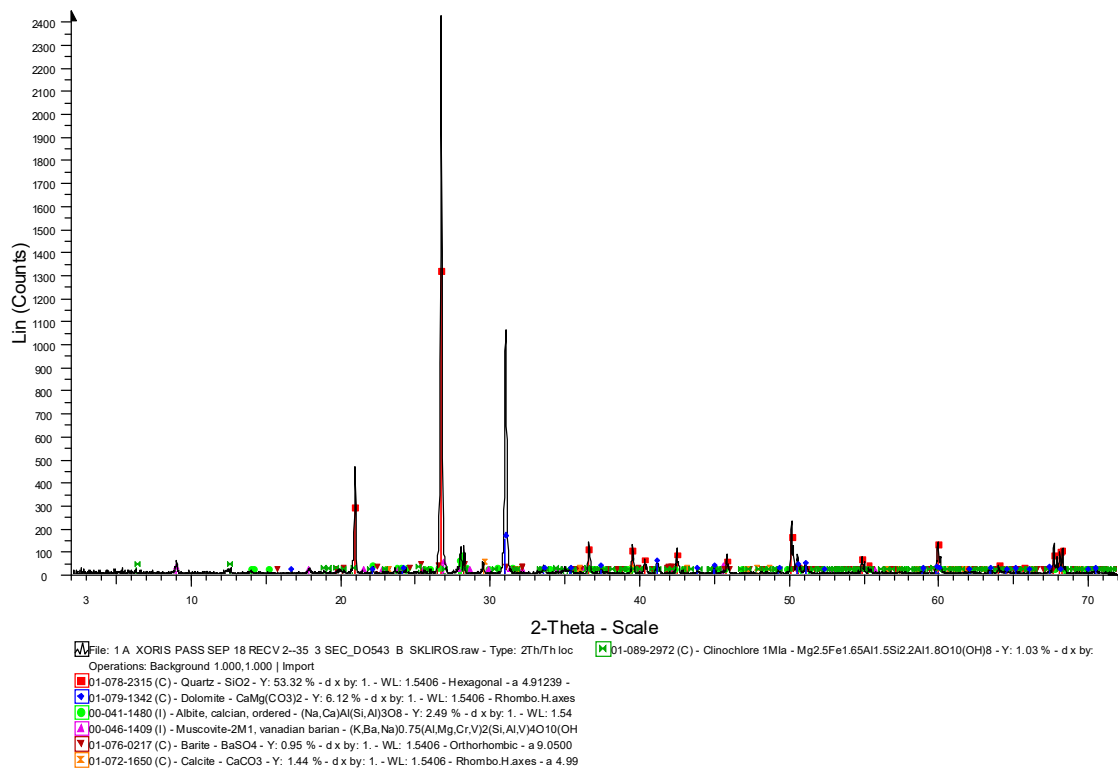


Figure S3: Representative XRD pattern of the fine-grained deposits found in Selinitsa cave.

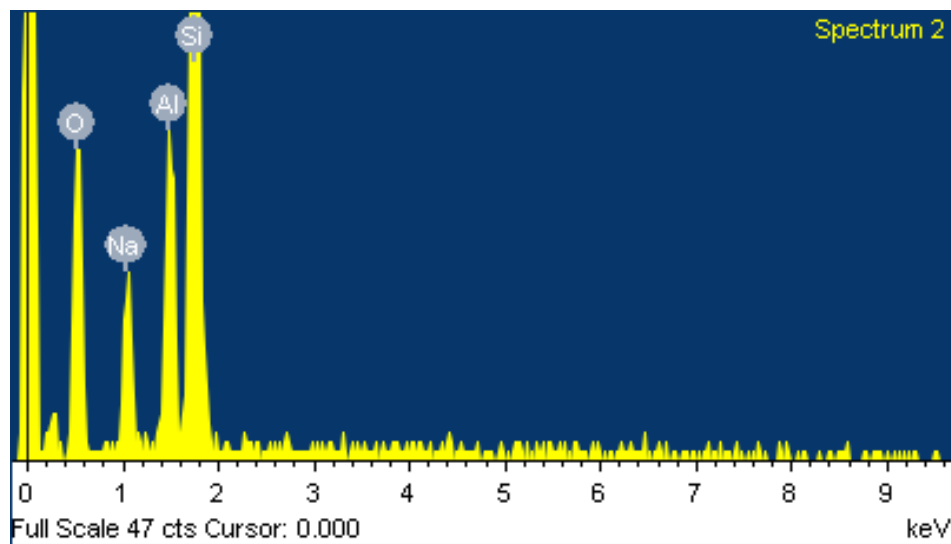


Figure S4. Representative SEM-EDS spectrum of detrital albite from the fine-grained deposits from Selinitsa cave.

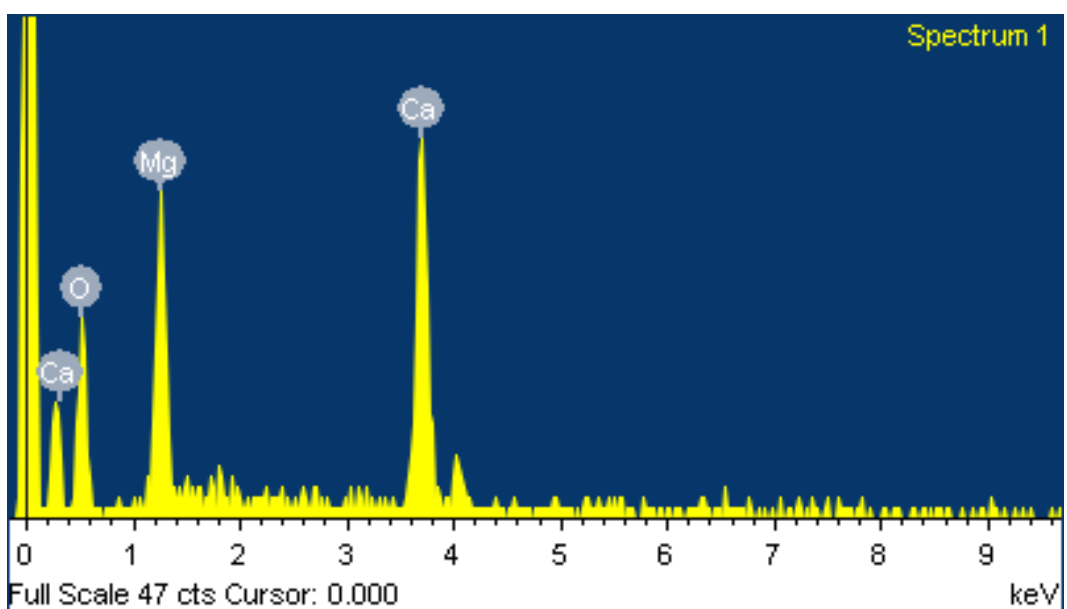
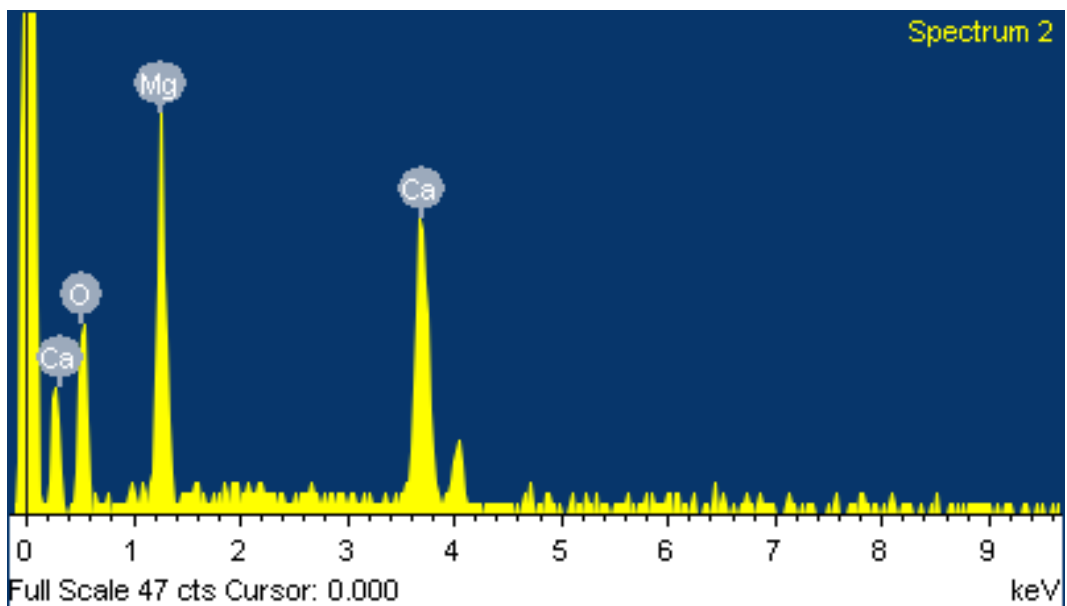


Figure S5. Representative SEM-EDS spectra of authigenic dolomite from the fine-grained deposits from Selinitsa cave.

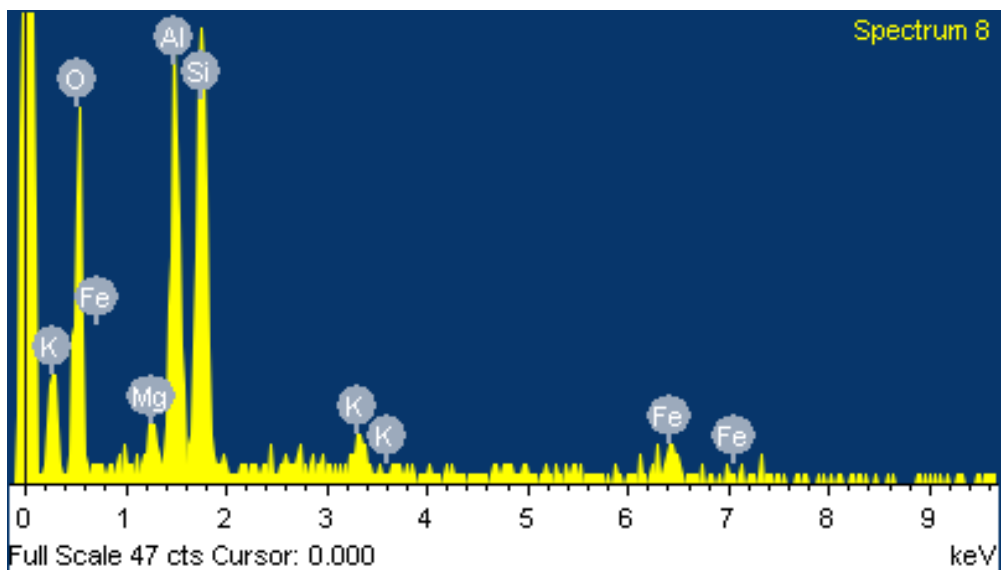


Figure S6. Representative SEM-EDS spectrum of detrital muscovite from the fine-grained deposits from Selinitsa cave.

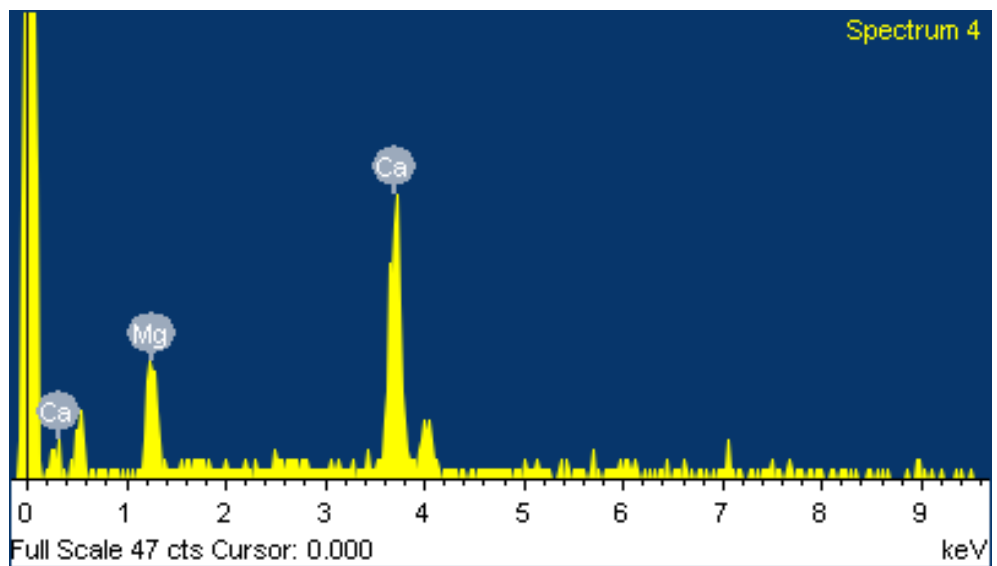


Figure S7. Representative SEM-EDS spectrum of Mg-calcite from the fine-grained deposits from Selinitsa cave.